Dispersion relations and speeds of sound in special sectors for the integrable chain with alternating spins

Dispersion relations and speeds of sound in special sectors for the integrable chain with alternating spins

B-D Dörfel† and St Meißner‡

Institut für Physik, Humboldt-Universität, Theorie der Elementarteilchen, Invalidenstraße 110, 10115 Berlin, Germany

Abstract. We investigate the anisotropic integrable chain consisting of spins $s = \frac{1}{2}$ and $s = 1$. Depending on the anisotropy and the ratio of the coupling constants it has different (antiferromagnetic) ground states, manifesting themselves in a different string content in the Bethe ansatz framework. In this paper we continue the study of those regions with different string content, below called sectors. First we compare the dispersion relations for the sectors with infinite Fermi zones. Further we calculate the speeds of sound for regions close to sector borders, where the Fermi radii either vanish or diverge, and compare the results.

1. Introduction

The integrable spin chain $XXZ(\frac{1}{2}, 1)$ constructed in 1992 by de Vega and Woynarovich [2] shows a rich physical structure with different ground states depending on the anisotropy parameter and the two coupling constants. In our previous papers [1, 3–5] we analysed this structure and calculated several important quantities. In this paper we deal mainly with dispersion relations and speeds of sound.

This is of special interest because in the model considered here several interesting features occur at the same time, while they have been observed before only seperately in different models. In [7], the occurrence of different gapless hole excitations with different velocities was first proved for the integrable XXZ Heisenberg model with arbitrary spin. In addition the situation changes drastically when spin and anisotropy are varied. Then the analogous effect was observed for models with more than one coupling constant: where the ground state and as a consequence the excitations depend on their ratios. Of peculiar interest were models of the class considered in [8], in which one excitation splits into two branches with different ('left' and 'right') speeds of sound due to non-symmetric dressed energy functions. This fact has been connected with the phenomenon of incommensurability.

We have established this splitting for two of our sectors [1]: for details see also sections 3 and 4. It is caused by the fact that the dressed energy function has a local maximum at zero (maintaining its symmetry), so that the filling starts with infinity rather than with zero. Exactly the same has been observed in an integrable generalized spin ladder model [9].

The paper is organized as follows. After reviewing the definitions in section 2 we remind the reader of the results of our last paper [1] concerning the phase diagram. In the same section the dispersion relations for all sectors with infinite Fermi zones only are compared. In section 4

---

† E-mail address: `doerfel@physik.hu-berlin.de`
‡ E-mail address: `meissner@qft2.physik.hu-berlin.de`

we present the calculations for the speeds of sound obtained either by power expansion or the Wiener–Hopf technique for small or large Fermi radii respectively.

Our conclusions are contained in section 5. Some useful definitions are compiled in the appendix.

2. Description of the model

We refer the reader to papers [2, 3] for the basics of the model.

Our Hamiltonian of a spin chain of length $2N$ is given by

$$\mathcal{H}(\gamma) = \bar{c}\bar{\mathcal{H}}(\gamma) + \tilde{c}\tilde{\mathcal{H}}(\gamma) \tag{2.1}$$

with the two couplings $\tilde{c}$ and $\bar{c}$. The anisotropy parameter γ is limited to $0 < \gamma < \pi/2$. For convenience we repeat the Bethe ansatz equations, the magnon energies and momenta and the spin projection.

$$\left(\frac{\sinh(\lambda_j + i\frac{\gamma}{2})}{\sinh(\lambda_j - i\frac{\gamma}{2})} \frac{\sinh(\lambda_j + i\gamma)}{\sinh(\lambda_j - i\gamma)} \right)^N = -\prod_{k=1}^{M} \frac{\sinh(\lambda_j - \lambda_k + i\gamma)}{\sinh(\lambda_j - \lambda_k - i\gamma)}, \qquad j = 1 \dots M \tag{2.2}$$

$$E = \bar{c}\bar{E} + \tilde{c}\tilde{E}$$

$$\bar{E} = -\sum_{j=1}^{M} \frac{2\sin\gamma}{\cosh 2\lambda_j - \cos\gamma}$$

$$\tilde{E} = -\sum_{j=1}^{M} \frac{2\sin 2\gamma}{\cosh 2\lambda_j - \cos 2\gamma} \tag{2.3}$$

$$P = \frac{i}{2} \sum_{j=1}^{M} \left\{ \log\left(\frac{\sinh(\lambda_j + i\frac{\gamma}{2})}{\sinh(\lambda_j - i\frac{\gamma}{2})} \right) + \log\left(\frac{\sinh(\lambda_j + i\gamma)}{\sinh(\lambda_j - i\gamma)} \right) \right\} \tag{2.4}$$

$$S_z = \frac{3N}{2} - M. \tag{2.5}$$

3. Phase structure and dispersion relations

In section 4 of [1] we carried out a complete analysis of the ground state structure based on the solution of the thermodynamic Bethe ansatz. We now review the main results.

Table 1. All sectors appearing in the phase diagram. Upper indices indicate infinite and finite Fermi zones. In the latter case, the second index distinguishes, whether the filling starts at $\lambda = 0$ or $\lambda = \infty$.

0	$(1, +)^{\infty}, (2, +)^{\infty}$
I	$(1, -)^{\infty}, (1, +)^{f,0}$
II	$(1, -)^{\infty}, (1, +)^{\infty}$
III	$(1, -)^{\infty}, (1, +)^{f,\infty}$
IV	$(1, -)^{\infty}$
V	$(1, -)^{\infty}, (2, +)^{f,0}$
VI	$(1, -)^{f,\infty}, (2, +)^{\infty}$

Using different sets of special anisotropy points we were able to prove that (for $0 < \gamma < \pi/2$) only three kinds of strings occur in the ground state. The picture changes remarkably at $\gamma = \pi/3$ and $\gamma = 2\pi/5$. All possible sectors are compiled in table 1 taken from [1]. To keep our notation consistent we found it useful to call the sector already discussed in [2] sector

0. In the $(\tilde{c}, \bar{c})$-plane the sector borders are straight lines starting from the origin. Moving anticlockwise from the $\tilde{c}$-axis the sectors follow in sequence 0, I, IV, V if $0 < \gamma \leqslant \pi/3$. For $\pi/3 < \gamma < 2\pi/5$ the sequence is 0, II, I, IV, VI and for $2\pi/5 < \gamma < \pi/2$ one has 0, II, III, IV, VI. In the case of $\gamma = 2\pi/5$, sector II is followed by IV and neither I or III occur. For details see figure 1 in [1].

From table 1 one can read, that the effect of velocity splitting mentioned in the introduction occurs in sectors III and VI for the $(1, +)$ and the $(1, -)$ strings, respectively. Therefore in both sectors we have three different speeds of sound instead of two: for details in sector III see in section 4.

To compare the dispersion relations in the sectors 0, II and IV it is convenient to work with the functions

$$p(\lambda, \alpha, \beta) = \arctan \frac{\sinh(\pi\lambda/\beta)}{\cos(\pi\alpha/2\beta)} \tag{3.1}$$

and

$$g(\lambda, \alpha, \beta) = \frac{4\pi}{\beta} \frac{\cos(\pi\alpha/2\beta)\cosh(\pi\lambda/\beta)}{\cosh(2\pi\lambda/\beta) + \cos(\pi\alpha/2\beta)}. \tag{3.2}$$

While p is odd, g is an even function of λ. Both are connected by

$$\frac{\mathrm{d}}{\mathrm{d}\lambda} p(\lambda, \alpha, \beta) = \tfrac{1}{2} g(\lambda, \alpha, \beta). \tag{3.3}$$

By straightforward calculation one may prove the relation

$$\sin\left(\frac{\pi}{2} + p(\lambda, \alpha, \beta)\right) \sqrt{\cos^2 p(\lambda, \alpha, \beta) + \frac{\sin^2 p(\lambda, \alpha, \beta)}{\cos^2(\pi\alpha/2\beta)}} = \frac{\beta}{2\pi} g(\lambda, \alpha, \beta). \tag{3.4}$$

We remark that in [4] we used a function $g(\lambda, \alpha)$ related by

$$g(\lambda, \alpha, \pi - \gamma) = g(\lambda, \alpha). \tag{3.5}$$

Let us first consider sector 0. The results are given in [2], taking into account our definition of momentum in equation (2.4). There are two elementary physical excitations: the holes in the distributions of the $(1, +)$- and $(2, +)$-strings respectively. We label them by index i, $i = 1, 2$.

$$p_h^i(\lambda = \lambda_h^i) = \frac{\pi}{4} + \frac{1}{2} p(\lambda, 0, \gamma) \tag{3.6}$$

$$\varepsilon_h^i(\lambda) = c^i \tfrac{1}{2} g(\lambda, 0, \gamma) \tag{3.7}$$

with $c^1 = \bar{c}$ and $c^2 = \tilde{c}$.

From equation (3.4) the dispersion relations follow

$$\varepsilon_h^i(p_h^i) = \frac{2\pi}{\gamma} c^i \frac{\sin 2p_h^i}{2}. \tag{3.8}$$

One may say that the dispersion relations diagonalize in the coupling constants. This fact changes in the other two sectors.

Next we look at sector IV which contains the case of negative couplings. The exact border lines are given in [5]. The elementary physical excitations are holes in the distribution of the $(1, -)$-strings. We quote the result from our paper [3], equations (4.5) and (4.6)

$$p_h(\lambda) = \frac{3\pi}{2} + \frac{1}{2} p(\lambda, 0, \pi - \gamma) + p(\lambda, \gamma, \pi - \gamma) \tag{3.9}$$

$$\varepsilon_h(\lambda) = -\frac{\bar{c}}{2} g(\lambda, 0, \pi - \gamma) - \tilde{c} g(\lambda, \gamma, \pi - \gamma). \tag{3.10}$$

The dispersion relation cannot be obtained in a closed form. One has to invert the monotone function (3.9) and substitute it in equation (3.10). Numerical calculations show a sine-like behaviour: see the broken curves in figure 2 of [3].

In [1] we found the new sector II, existing only for $\gamma > \pi/3$ (for the exact border lines see section 4). Here the excitations are $(1, +)$- and $(1, -)$-string holes. The dispersion law for the $(1, -)$-string holes is simple:

$$p_h^{1-}(\lambda) = \frac{\pi}{4} + \frac{1}{2} p(\lambda, 0, \pi - 2\gamma) \tag{3.11}$$

$$\varepsilon_h^{1-}(\lambda) = -\frac{\tilde{c}}{2} g(\lambda, 0, \pi - 2\gamma) \tag{3.12}$$

$$\varepsilon_h^{1-}(p_h^{1-}) = -\frac{2\pi\tilde{c}}{\pi - 2\gamma} \frac{\sin 2p_h^{1-}}{2}. \tag{3.13}$$

To write down the case of $(1, +)$-strings it is necessary to introduce a new function $d_1(\lambda)$

$$d_1(\lambda) = \frac{1}{2\pi} \int_{-\infty}^{\infty} e^{i\omega\lambda} \frac{\cosh(\omega(\pi - 3\gamma)/2)\mathrm{d}\omega}{2\cosh(\omega(\pi - 2\gamma)/2)\cosh(\omega\gamma/2)} \tag{3.14}$$

already used in [1]. We further define another function $e_1(\lambda)$ by

$$\frac{\mathrm{d}}{\mathrm{d}\lambda} e_1(\lambda) = d_1(\lambda) \quad \text{and} \quad e_1(0) = 0. \tag{3.15}$$

$$p_h^{1+} = \frac{\pi}{2} + \frac{1}{2} p(\lambda, 0, \gamma) + 2\pi e_1(\lambda) \tag{3.16}$$

$$\varepsilon_h^{1+} = \bar{c}\frac{1}{2} g(\lambda, 0, \gamma) + 2\pi\tilde{c}d_1(\lambda). \tag{3.17}$$

We have calculated the dispersion law numerically and show the results in figure 1. It is interesting to look closer at the point $\gamma = 2\pi/5$, where the function $d_1(\lambda)$ simplifies and becomes $1/4\pi g(\lambda, 0, \gamma)$, resulting in the simple dispersion law

$$\varepsilon_h^{1+} = \frac{2\pi}{\gamma} \frac{\bar{c} + \tilde{c}}{2} \sin p_h^{1+}. \tag{3.18}$$

All dispersion laws possess a symmetry connected with the properties of the functions $p_h(\lambda)$ and $\varepsilon_h(\lambda)$:

$$p_h(\lambda) = p_0 + \bar{p}(\lambda) \quad \text{and} \quad \bar{p}(-\lambda) = -p(\lambda) \tag{3.19}$$

$$\varepsilon_h(\lambda) = \varepsilon_h(-\lambda). \tag{3.20}$$

One then derives easily

$$\varepsilon_h(p_h) = \varepsilon_h(2p_0 - p_h). \tag{3.21}$$

In addition one has $0 \leqslant p_h \leqslant 2p_0$. The constants $2p_0$ are different, so in sector 0 they are $\pi/2$ for both excitations; the same is true for the negative parity excitation in II. The other (positive parity) excitation in II has $2p_0 = \pi$, while in IV one has $2p_0 = 3\pi/2$.

There is a general rule for the sum of those constants in every sector being $3\pi/2$ (due to antiferromagnetic ground state), but excitations containing more than one magnon, e.g. $(2, +)$-strings, must be taken with their appropriate multiplicity.

4. The speed of sound in different sectors

In this section we present some calculations for the speed of sound in sectors with one finite Fermi radius (the other one stays infinite), where this radius is either small or large, so that an approximation can be made. On the other hand, that gives just the values of the speed near to
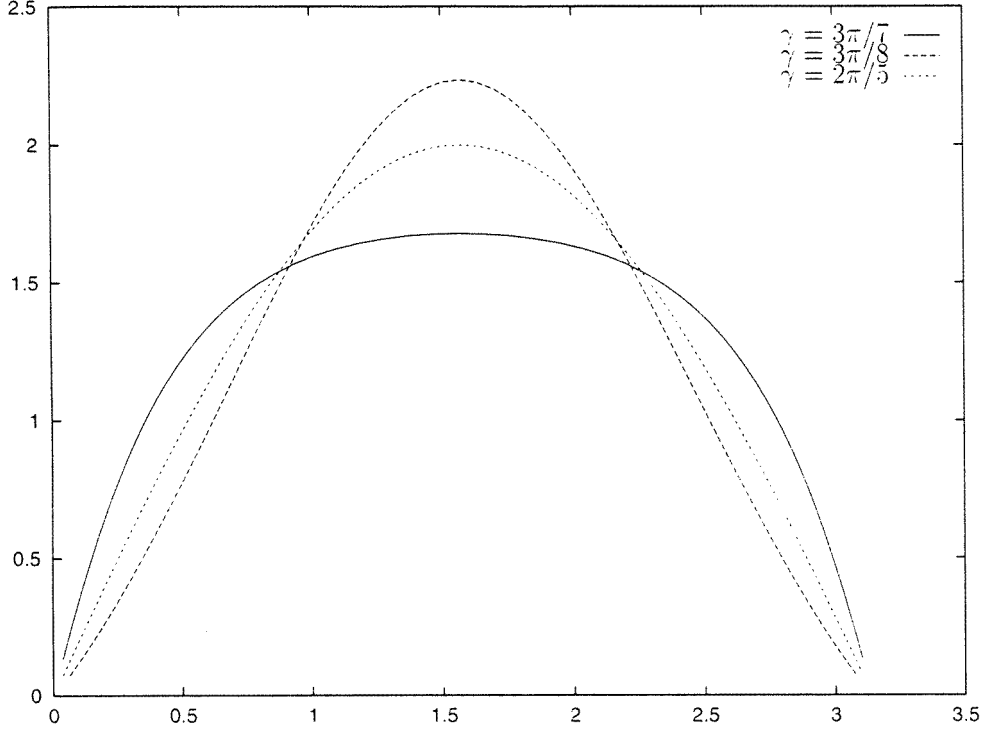
Figure 1. Dispersion relations for the holes in the $(1, +)$-string distributions in sector II for $\bar{c} = -5\tilde{c} = 1$ and different γ.

the border lines of the above-mentioned sector which might be of interest for understanding the physics of the model. We limit our calculations to the case $\bar{c} > 0$, $\tilde{c} < 0$. Thus, the sectors in question are I and III. Sectors V and VI could be treated in an analogous way.

We start with sector I. The equations of the thermodynamic Bethe ansatz can be taken from [1] (equation (4.5)).

$$\epsilon_{1+}(\lambda) = -2\pi\bar{c}s_1(\lambda) - 2\pi\tilde{c}d_1(\lambda) + d_1 * \epsilon_{1+}^+(\lambda) \tag{4.1}$$

$$\epsilon_{1-}(\lambda) = 2\pi\tilde{c}s_2(\lambda) - s_2 * \epsilon_{1+}^+(\lambda). \tag{4.2}$$

Here $\varepsilon_i(\lambda)$ are the dressed energies. Their lower index specifies the excitation, while the upper stands for the positive and negative parts respectively. The convolution is defined by

$$a * b(\lambda) = \int_{-\infty}^{\infty} d\mu\, a(\lambda - \mu)b(\mu). \tag{4.3}$$

(For $s_1(\lambda)$ and $s_2(\lambda)$ see the appendix.)

Restricting γ by $0 < \gamma < 2\pi/5$ we consider the case

$$0 < \beta = \bar{c} - \frac{|\tilde{c}|}{2\cos\tilde{\gamma}} \ll 1 \tag{4.4}$$

with the usual definition $\tilde{\gamma} = \pi\gamma/2(\pi - \gamma)$.

From equation (3.13) from [4] we know that $\beta = 0$ describes the border line between sectors IV and I.

To employ the method of power expansions in the (small) Fermi radius b of the $(1, +)$-strings, it is useful to reformulate equations (4.1) and (4.2) in the way

$$\varepsilon_{1+}(\lambda) = -\bar{c}g(\lambda, \pi - 2\gamma) - \tilde{c}g(\lambda, \pi - 3\gamma) - \frac{1}{2\pi}g(\lambda, \pi - 3\gamma) * \varepsilon_{1+}^-(\lambda) \tag{4.5}$$

$$\varepsilon_{1-}(\lambda) = 2\pi\bar{c}s_1(\lambda) + \tilde{c}g(\lambda, \gamma) + \frac{1}{2\pi}g(\lambda, \gamma) * \varepsilon_{1+}^-(\lambda). \tag{4.6}$$

Equation (4.5) determines the Fermi radius b: in lowest order the convolution term can be neglected and b is given by $\varepsilon_{1+}(b) = 0$. The derivative $d\varepsilon/dp$ is calculated as (see equation (5.1) in [1])

$$\frac{d\varepsilon}{dp} = \frac{d\varepsilon}{d\lambda}\frac{d\lambda}{dp} = -\frac{d\varepsilon}{d\lambda}\frac{2}{\varepsilon(\lambda)}\bigg|_{\bar{c}=\tilde{c}=1}. \tag{4.7}$$

The speed of sound is then given if λ is put equal to b.

After rather long technical calculations we obtain

$$v_{1+} = \frac{4\pi}{\pi - \gamma}\frac{1}{\sin\tilde{\gamma}}\sqrt{\frac{2\cos\tilde{\gamma} - 1}{2\cos\tilde{\gamma} + 1}}(\bar{c}\beta)^{1/2}. \tag{4.8}$$

Using equation (4.6) in the same way gives

$$v_{1-} = \frac{2\pi}{\pi - \gamma}(2\cos\tilde{\gamma} - 1)\bar{c} + \frac{8}{\pi - \gamma}\sin\tilde{\gamma}\sqrt{\frac{2\cos\tilde{\gamma} - 1}{2\cos\tilde{\gamma} + 1}}(\bar{c}\beta)^{1/2}. \tag{4.9}$$

Here the first term is just the limiting value on the border of sector IV.

Next we consider $\pi/3 < \gamma < 2\pi/5$ and look for the border of sector I with sector II (see [1], equation (4.10)). It is given by

$$0 < \alpha = |\tilde{c}|\tan\left(\frac{\pi^2}{2\gamma}\right) - \bar{c} \ll 1. \tag{4.10}$$

Then equation (4.1) is of Wiener–Hopf type and can be solved explicitly for large b giving

$$v_{1+} = \frac{2\pi}{\gamma}\frac{3\gamma - \pi}{\pi - 2\gamma}\frac{\alpha}{1 + \tan\left(\frac{\pi^2}{2\gamma}\right)}. \tag{4.11}$$

From equation (4.2) one has to extract the asymptotics of $\varepsilon_{1-}(\lambda)$ for large λ (the Fermi radius is infinite). The first term on the RHS gives the limiting value of v_{1-} on the border of sector II (it is non-vanishing). Remarkably for $\alpha > 0$ the asymptotics is always given by the second term with the convolution. So the result is of the same order in α as v_{1+}:

$$v_{1-} = \frac{2\pi}{\gamma}\frac{3\gamma - \pi}{\gamma}\frac{\alpha}{1 + \tan\left(\frac{\pi^2}{2\gamma}\right)}. \tag{4.12}$$

Therefore v_{1-} shows a discontinuity on the border I/II.

After sector I we consider sector III. Then one has $2\pi/5 < \gamma < \pi/2$. We start again with the border to sector IV.

$$0 < \beta' = \bar{c} - 2\cos\tilde{\gamma}\tilde{c} \ll 1. \tag{4.13}$$

The Fermi radius is determined again from equation (4.5), but now instead of power expansion we have to solve a Wiener–Hopf problem due to the fact that b is large. The calculation is straightforward after realizing that for the positive frequency part of the inhomogeneous function one has to take into account the dominant two poles (instead of one). As already mentioned in [1] the fact that filling of the $(1, +)$-strings starts at infinity causes the appearance

of two velocities for them taken at $\lambda = b$ and $\lambda = \infty$. While the calculations for both are different, the results coincide in first order.

The same happens for v_{1-} calculated from the asymptotics of equation (4.6). We remind the reader that v_{1-} vanishes at the border. Finally we have obtained

$$v_{1+}^{(1)} = v_{1+}^{(2)} = v_{1-} = \frac{2\pi}{\pi - \gamma} \frac{\beta'}{1 + 2\cos\tilde{\gamma}}. \tag{4.14}$$

We have no explanation for this striking fact, that all velocities are equal in first order. Nevertheless we are sure that the effect does not survive in higher order.

To close this part we have to consider the border line with sector II (see [1], equation (4.8)).

$$0 < \alpha' = |\tilde{c}| 2\gamma d_1(0) - \bar{c} \ll 1. \tag{4.15}$$

The Fermi radius b is determined by equation (4.1) using power expansion. The calculation is straightforward, but rather tedious because of the presence of the function $d_1(\lambda)$. But the order of magnitude can be estimated easily. The two velocities $v_{1-}^{(1)}$ and $v_{1+}^{(2)}$ (taken at $\lambda = \infty$) obtain corrections to their (constant) limiting values from sector II of the order $\sqrt{\alpha'}$. The third velocity $v_{1+}^{(1)}$ (taken at $\lambda = b$) is of order $\sqrt{\alpha'}$.

We did not consider the border of sectors I and 0 for $0 < \gamma \leqslant \pi/3$ because both sectors are separated form each other by a singular line with a highly degenerate ground state which is different from the other lines considered above.

5. Conclusions

First we make some general comments on the character of the behaviour of the velocities considered. We parametrize the coupling constants by two parameters: one c, setting the energy scale (below put to one); the other an angle φ, which describes their ratio.

$$\begin{aligned} \bar{c} &= c\sin\varphi \\ \tilde{c} &= c\cos\varphi. \end{aligned} \tag{5.1}$$

From our results in section 4 one can see that, in general, the behaviour near the sector borders is either linear or a square root in cosine/sine-functions of φ. Which behaviour emerges is determined by the radius b. Large b produces Wiener–Hopf equations and linear behaviour, small b causes power expansions and a square root behaviour. Considering sector I only, one could superficially conclude that this depends only on the sector on the other side of the border. Our analysis in sector III shows that the situation reverses with respect to sector I.

In just one case we have found a discontinuity of one of the velocities when a sector border is passed (see equation (4.12)). It is the case for v_{1-} on the border I/II. Nothing of this kind happens for sector III, because for small α' we have power expansion, which is incapable of producing such an effect. On the other hand (for small β'), v_{1-} vanishes on the other side of the border in sector IV. In general, one would expect a discontinuity only when a singular line is crossed which means that an excitation with an infinite Fermi zone disappears at once (see below). It is instructive to compile all analytically calculated velocities in one picture at the special point $\gamma = 2\pi/5$, which we have done in figure 2.

For convenience, we have given the analytical shape in the various sectors in table 2. Looking at figure 2 one clearly sees two effects. First, the two singularity lines at $\varphi = \pi/2$ (the vanishing of the $(2, +)$-strings) and at $\varphi = 3\pi/4$ (the vanishing of the $(1, +)$-strings) cause discontinuities for the speed of the remaining excitation. While the first line is universal for arbitrary γ, the second one is peculiar to $\gamma = 2\pi/5$. For other γ that line is replaced by sectors I or III.
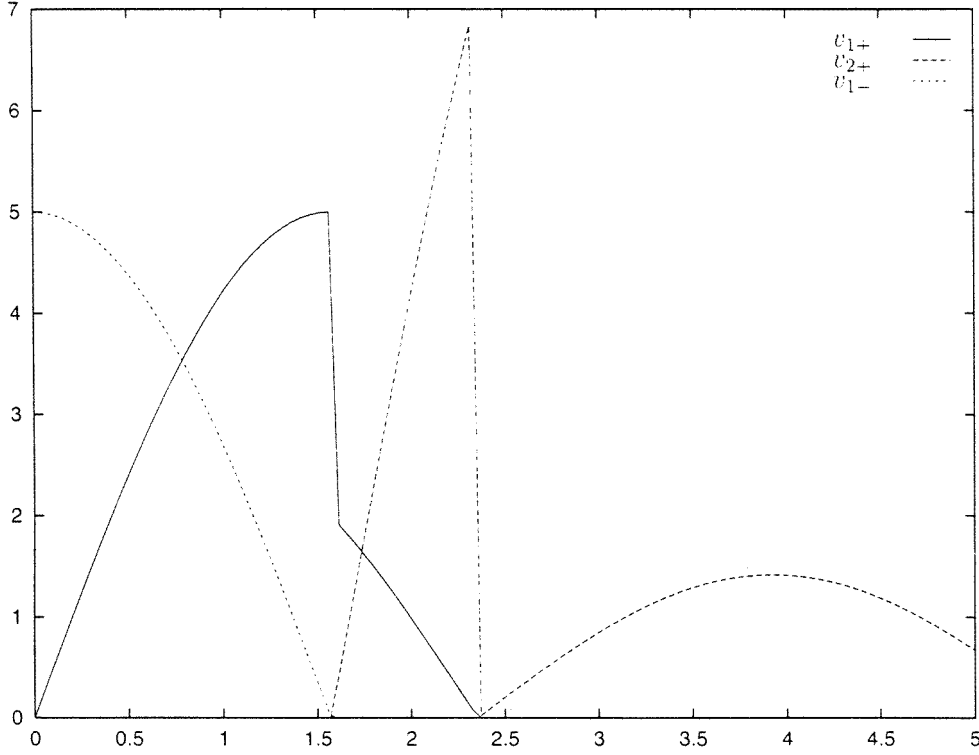
Figure 2. The speeds of sound as functions of the angle φ for $\gamma = 2\pi/5$ and those sectors where all speeds of sound are known.

Table 2. The speeds of sound and the sector borders as functions of the angle φ for $\gamma = 2\pi/5$.

Sectors	0	II	IV	V
Borders	$0, \pi/2$	$\pi/2, 3\pi/4$	$3\pi/4, 2\pi - \arctan 4$	$2\pi - \arctan 4, 2\pi$
v_{1+}	$5\sin\varphi$	$5/2\sin\varphi + 5/2\cos\varphi$	0	0
v_{2+}	$5\cos\varphi$	0	0	
v_{1-}	0	$-10\cos\varphi$	$-5/3\sin\varphi - 5/3\cos\varphi$	

Second, one sees the two conformal points where two velocities intersect, one at $\varphi = \pi/4$ and the other at $\varphi = \pi - \arctan 5$ [4].

Our calculations in the previous section allow us now to look more closely at what happens for $\pi/3 < \gamma < 2\pi/5$ when the above-mentioned singularity line is replaced by sector I. As far as the limits of sectors II and IV are concerned, the only change is that v_{1-} no longer vanishes at the border of sector IV. Now we make use of equations (4.9)–(4.12). They tell us, first, that both velocities must reach their maximum (at different φ) within sector I and, second, that there is at least one point of intersection in the same sector. At that point the finite size corrections must exhibit a rather simple structure, as in [6].

We conjecture that there is no such effect in sector III but a strict proof will require further calculations. Our calculations also show another interesting effect: at $\beta' = 0$ all velocities vanish.

Finally we remark that we expect the theory at $\gamma = 2\pi/5$ and with both velocities equal to be highly symmetric and of particular interest. Up to now it is only known that its central charge is two. We were not able to calculate the operator dimensions analytically, because unlike in [5], it requires knowledge of the dressed charge [6] and hence the explicit factorization of the kernel.

Acknowledgment

The authors would like to thank H Frahm for helpful discussions.

Appendix

$$s_1(\lambda) = \frac{1}{2\gamma \cosh(\pi\lambda/\gamma)}$$

$$s_2(\lambda) = \frac{1}{2(\pi - 2\gamma)\cosh(\pi\lambda/(\pi - 2\gamma))}$$

$$g(\lambda, \alpha) = \int_{-\infty}^{\infty} \mathrm{e}^{\mathrm{i}\omega\lambda} \frac{\cosh\omega\alpha/2}{\cosh\omega(\pi - \gamma)/2}\,\mathrm{d}\omega.$$

References

[1] Dörfel B-D and Meißner St 1998 *J. Phys. A: Math. Gen.* **31** 61
[2] de Vega H J and Woynarovich F 1992 *J. Phys. A: Math. Gen.* **25** 4499
[3] Meißner St and Dörfel B-D 1996 *J. Phys. A: Math. Gen.* **29** 1949
[4] Dörfel B-D and Meißner St 1996 *J. Phys. A: Math. Gen.* **29** 6471
[5] Dörfel B-D and Meißner St 1997 *J. Phys. A: Math. Gen.* **30** 1831
[6] Woynarovich F 1989 *J. Phys. A: Math. Gen.* **22** 4243
[7] Kirillov A N and Reshetikhin N Yu 1987 *J. Phys. A: Math. Gen.* **20** 1565
[8] Tsvelick A M 1990 *Phys. Rev.* B **42** 779
    Frahm H 1992 *J. Phys. A: Math. Gen.* **25** 1417
[9] Frahm H and Rödenbeck C 1997 *J. Phys. A: Math. Gen.* **30** 4467